

Effect of Multiple H-Bonding on the Properties of Polyimides Containing the Rigid Rod Groups

Xiaoye Ma, Chuanqing Kang, Wenhui Chen, Rizhe Jin, Haiquan Guo, Xuepeng Qiu, Lianxun Gao

State Key Laboratory of Polymer Physics and Chemistry, Changchun Institute of Applied Chemistry, Chinese Academy of Sciences, Changchun, 130022, People's Republic of China

Correspondence to: X. Ma (E-mail: xyma@ciac.jl.cn) or L. Gao (E-mail: lxgao@ciac.jl.cn)

Received 28 May 2015; accepted 24 July 2015; published online 28 August 2015

DOI: 10.1002/pola.27808

ABSTRACT: To investigate the influence of hydrogen bonding on the properties of polyimides (PIs) containing rigid rod-like groups, five symmetrical diamines containing benzimidazole, benzoxazole, and hydroxy group were synthesized, and then a series of PIs were prepared. Results showed that hydroxyl-containing poly(benzoxazole imide)s possess higher glass transition temperature (T_g) and dimensional stabilities than their corresponding poly(benzoxazole imide)s. Moreover, the corresponding poly(benzimidazole imide)s presented the best performances, such as the highest T_g , the highest char yield and

the highest dimensional stabilities. The influence of hydrogen bonding of benzimidazole on the properties of PIs was stronger than that of hydroxyl groups. Hydroxyl-containing poly(benzoxazole imide)s were formed in crosslinking structures after heat treatment at 400 °C. © 2015 Wiley Periodicals, Inc. *J. Polym. Sci., Part A: Polym. Chem.* **2016**, *54*, 570–581

KEYWORDS: benzimidazole; benzoxazole; hydrogen bonding; intra-/intermolecular interaction; polyimides; rigid rod groups

INTRODUCTION Aromatic polyimides (PIs), as commercialized aromatic heterocyclic polymers, are widely used in the semiconductor and electronic packaging industries because of their outstanding thermal stability, excellent insulation properties, low dielectric constant, good adhesion to common substrates, and superior chemical stability.^{1–4} The outstanding properties of PIs are mainly dependent on the chemical structure, molecular aggregation, and intra-/intermolecular interaction. In our previous work, the rigid rod-like pyridine-containing diamines, 2,5-bis(4-aminophenyl)pyridine and 2-(4-aminophenyl)-5-aminopyridine, were introduced into the backbone of PI, and the thermal and mechanical properties were increased significantly.⁵ The PIs can be enhanced in the original properties by introducing rigid rod-like nitrogen heterocyclic structure.

Aromatic polybenzoxazoles (PBOs) and polybenzimidazoles (PBIs) exhibit excellent mechanical properties and thermal stability due to the rigidity of polymer backbones, aromatic heterocyclic chemical structures, and strong intermolecular associations.^{6,7} However, PBOs and PBIs are generally difficult to process because of their unmeltable behavior and poor solubility in conventional organic solvents, thus limiting their potential applications. This problem is circumvented in

PIs, especially in thin-film formation, through the processing of soluble poly(amic acid) intermediates. Meanwhile, it can be predicted that incorporating rigid-rod benzoxazoles and benzimidazoles into PI main chains can effectively improve the thermal and mechanical properties of PIs. In recent years, many research have been carried out to develop new promising systems of high-performance materials by combining the advantages of PIs, PBOs, and PBIs.^{8–24} For instance, the asymmetrical diamines 5,4'-diamino-2-phenyl benzimidazole²² and 5,4'-diamino-2-phenyl benzoxazole²³ were incorporated into PI main chains, and the thermal and mechanical properties of the resultant PI films were remarkably enhanced in comparison with those of common PI films.

Hydrogen bonding (H-bonding) is a kind of intermolecular interaction, and performs a crucial function to improve the properties of rigid polymers. There is no H-bonding interaction between molecular chains in the conventional aromatic PIs. In recent years, the H-bonding interaction of benzimidazole in rigid PIs has been researched. The —NH— group of benzimidazole can form H-bonding with the C=O of the imide ring in the PIs containing benzimidazole, and improve the properties of PIs.^{24,25} Previous reports indicated that the incorporation of hydroxyl groups can also form H-bonding

Additional Supporting Information may be found in the online version of this article.

© 2015 Wiley Periodicals, Inc.

and enhance the properties of high-performance fibers, among others, like M5 fibers,^{26,27} but the H-bonding of hydroxyl group in rigid PIs has not been reported.

In this study, five fully symmetrical diamines containing benzimidazole, benzoxazole, and hydroxyl group were synthesized, and then a series of PIs were prepared by the reaction of these diamines with commercial aromatic dianhydrides. The influences on the properties of PIs by the introduction of rigid rod-like nitrogen heterocyclic structure and the formation of intra-/intermolecular H-bonding were discussed.

EXPERIMENTAL

Materials

4,6-Diaminoresorcinol dihydrochloride (Zhejiang Jiangnan Pharmaceutical Factory), 4-aminobenzoic acid (Adamas Reagent Co., Ltd.), 4-aminosalicylic acid (Adamas Reagent Co., Ltd.), 3,3'-diaminobenzidine (Shanghai Zhuorui Chemical Co., Ltd.), and 3,3'-dimethoxybenzidine dihydrochloride (Shanghai Zhuorui Chemical Co., Ltd.) were purchased and directly used. 3,3',4,4'-Biphenyl tetracarboxylic dianhydride (BPDA), 4,4'-oxydiphthalic dianhydride (ODPA), and 3,3',4,4'-benzophenone tetracarboxylic dianhydride (BTDA) were obtained by sublimation under vacuum. 1,4-Bis(3,4-dicarboxyphenoxy)benzene dianhydride (HQDPA, prepared in our laboratory) was purified by dehydration of acetic anhydride. *N,N*-dimethylacetamide (DMAc) and *N*-methyl-2-pyrrolidinone (NMP) were distilled under reduced pressure before use. Other common reagents were purchased from commercial sources and used as received.

Characterization

¹H and ¹³C nuclear magnetic resonance (NMR) spectra were recorded on a Bruker 400 spectrometer at 400 MHz and with tetramethylsilane as an internal standard. Inherent viscosities were measured with 0.5 g/dL concentration of poly(amic acid)s (PAAs) in DMAc using an Ubbelohde viscometer at 30 °C. Thermogravimetric analyses (TGAs) were performed at a heating rate of 10 °C/min under nitrogen with a Perkin Elmer Pyris Diamond TG/DTA. Dynamic mechanical analysis (DMA) was carried out with a TA instrument DMA Q800 at a heating rate of 5 °C/min and a load frequency of 1 Hz in film tension geometry in nitrogen atmosphere, and glass transition temperature (T_g) was regarded as the peak temperature of the $\tan \delta$ curve. Small-angle and wide-angle X-ray diffraction (XRD) patterns were obtained using a Bruker D8 ADVANCE XRD with Cu-K radiation at a wavelength (λ) 1.54 Å. The dimensional stability of the films was investigated using a TMA Q400 thermal mechanical analyzer; film samples sized 2 mm × 4 cm, and with an initial tension of 0.05 N.

Synthesis of Diamines

In a 1000 mL three-necked flask, 4,6-diaminoresorcinol dihydrochloride (12.78 g, 0.06 mol) and 4-aminobenzoic acid (16.46 g, 0.12 mol) were dissolved in 120 g of poly(phosphoric acid) (PPA) under a nitrogen atmosphere to produce

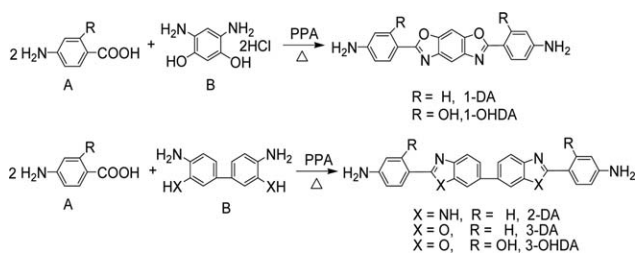
a thick paste. The mixture was slowly heated to 110 °C to inhibit excessive foaming and then continuously stirred for 2 h at 110 °C. The temperature was slowly increased to 200 °C and then maintained for 6 h. The reaction mixture was then slowly cooled to 100 °C and poured into ice-cold water with rapid stirring. The precipitate was collected by filtration and soaked overnight in a sodium bicarbonate solution. The precipitate was collected, thoroughly washed with water, and dried under vacuum at 80 °C. The crude product, 1-DA, was further purified by sublimation. TOF-MS: m/z = 342.1. ¹H NMR (400 MHz, DMSO-*d*₆) δ (ppm): 8.06(s, 1H, Ar-H), 7.86–7.88 (m, 5H, Ar-H), 6.72, 6.70 (d, 4H, Ar-H), 5.99 (s, 4H, NH₂). ¹³C NMR (100 MHz, DMSO-*d*₆) δ (ppm): 164.3, 152.8, 147.6, 139.9, 129.2, 113.9, 113.1, 107.4, 93.6.

Diamine (1-OHDA) was synthesized in a procedure similar to that of 1-DA, but using 4,6-diaminoresorcinol dihydrochloride and 4-aminosalicylic acid as starting materials. TOF-MS: m/z = 374.1. ¹H NMR (400 MHz, DMSO-*d*₆) δ (ppm): 11.07 (s, 2H, —OH), 8.15(s, 1H, Ar-H), 7.91 (s, 1H, Ar-H), 7.66, 7.64 (d, 2H, Ar-H), 6.29–6.31 (m, 2H, Ar-H), 6.201, 6.197 (d, 2H, Ar-H), 6.09 (s, 4H, NH₂). ¹³C NMR (100 MHz, DMSO-*d*₆) δ (ppm): 164.5, 159.9, 154.9, 146.0, 138.0, 128.6, 107.6, 105.9, 99.6, 98.2, 94.1.

In a 500 mL three-necked flask, 3,3'-dihydroxy-4,4'-diaminobiphenyl (5.0 g, 0.023 mol) and 4-aminobenzoic acid (6.342 g, 0.046 mol) were dissolved in 80 g of PPA under a nitrogen atmosphere to produce a thick paste. The mixture was slowly heated to 200 °C and then maintained for 6 h. Then, the reaction mixture was slowly cooled to 100 °C and poured into ice-cold water with rapid stirring. The precipitate was collected by filtration and soaked overnight in a sodium bicarbonate solution. The precipitate was collected, thoroughly washed with water, and dried under vacuum at 80 °C. The crude product, 3-DA, was further purified by recrystallization from DMAc/H₂O. TOF-MS: m/z = 418.1. ¹H NMR (400 MHz, DMSO-*d*₆) δ (ppm): 8.02 (s, 2H, Ar-H), 7.88, 7.86 (d, 4H, Ar-H), 7.70 (s, 4H, Ar-H), 6.71, 6.68 (d, 4H, Ar-H), 5.99 (s, 4H, NH₂). ¹³C NMR (100 MHz, DMSO-*d*₆) δ (ppm): 164.2, 152.6, 150.7, 141.6, 136.4, 129.0, 123.7, 118.8, 113.6, 112.6, 108.6.

Diamine (2-DA) was synthesized in a procedure similar to that of 3-DA, but with 3,3'-diaminobenzidine and 4-aminobenzoic acid as starting materials. TOF-MS: m/z = 416.2. ¹H NMR (400 MHz, DMSO-*d*₆) δ (ppm): 12.46 (s, 2H, imidazole, —NH), 7.87, 7.85(d, 4H, Ar-H), 7.70(s, 2H, Ar-H), 7.54 (s, 2H, Ar-H), 7.44, 7.42 (d, 2H, Ar-H), 6.68, 6.66 (d, 4H, Ar-H), 5.60 (s, 4H, NH₂). ¹³C NMR (100 MHz, DMSO-*d*₆) δ (ppm): 153.4, 150.9, 135.5, 128.1, 121.3, 117.6, 113.9.

Diamine (3-OHDA) was synthesized in a procedure similar to that of 3-DA, but with 3,3'-dihydroxy-4,4'-diaminobiphenyl and 4-aminosalicylic acid as starting materials. TOF-MS: m/z = 450.1. ¹H NMR (400 MHz, DMSO-*d*₆) δ (ppm): 11.13 (s, 2H, —OH), 8.10 (s, 2H, Ar-H), 7.75 (s, 4H, Ar-H), 7.68, 7.65 (d, 2H, Ar-H), 6.31, 6.29 (d, 2H, Ar-H), 6.19 (d, 2H, Ar-H), 6.11 (s, 4H, NH₂). ¹³C NMR (100 MHz, DMSO-*d*₆) δ (ppm): 164.1, 159.9,



SCHEME 1 Synthesis of diamines.

154.7, 149.1, 139.5, 136.5, 128.4, 124.2, 118.0, 108.8, 107.3, 99.3, 97.8.

Synthesis of PIs

PIs were prepared using a conventional two-stage solution polymerization and imidization process. The polymerization of 3-BPPI is described here as a typical example: BPDA (0.4413 g, 1.5 mmol), 3-DA (0.6272 g, 1.5 mmol), and 15 mL DMAc were placed in a 100 mL three-necked flask equipped with a mechanical stirrer and a nitrogen inlet. The mixture was stirred at room temperature for 8 h to form a viscous solution of PAA with a solid content of 7 wt %.

A film was cast from the PAA solution onto a flat glass plate and dried at 50 °C for 12 h. Then, a programmed procedure in a ventilated oven at 80 and 140 °C for 1 h, respectively, was used to remove residual solvents. The plate was placed into a vacuum oven and treated at 200, 250, 300, and 350 °C for 1 h, respectively, to obtain a fully imidized film. The polymer films were easily stripped off from the glass plate by soaking in water.

RESULTS AND DISCUSSION

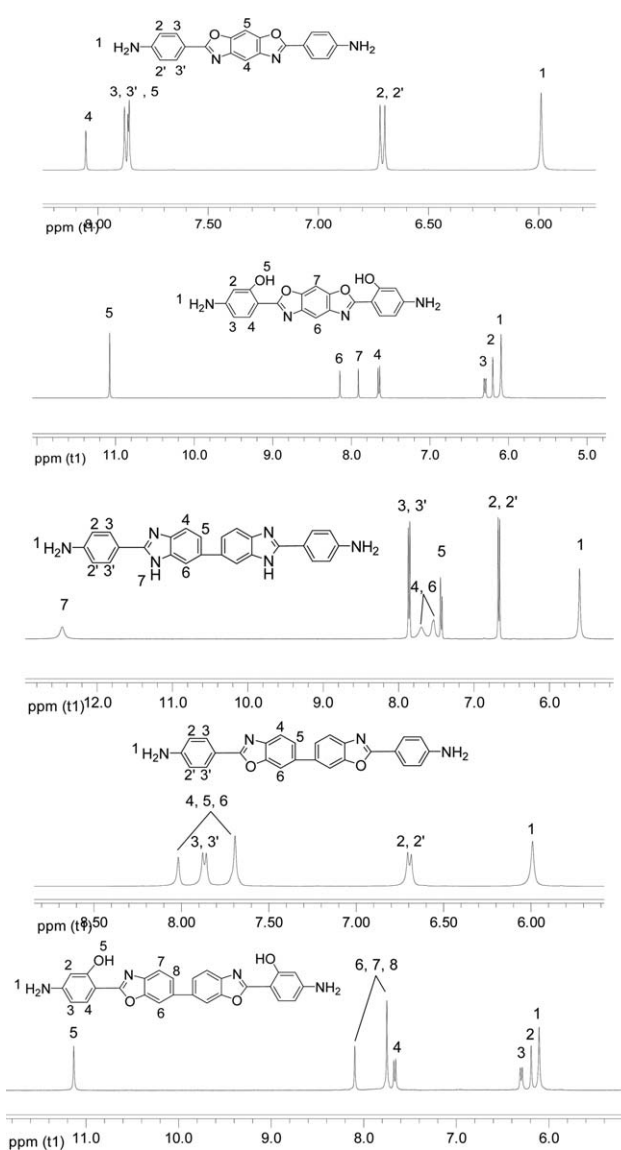
Synthesis

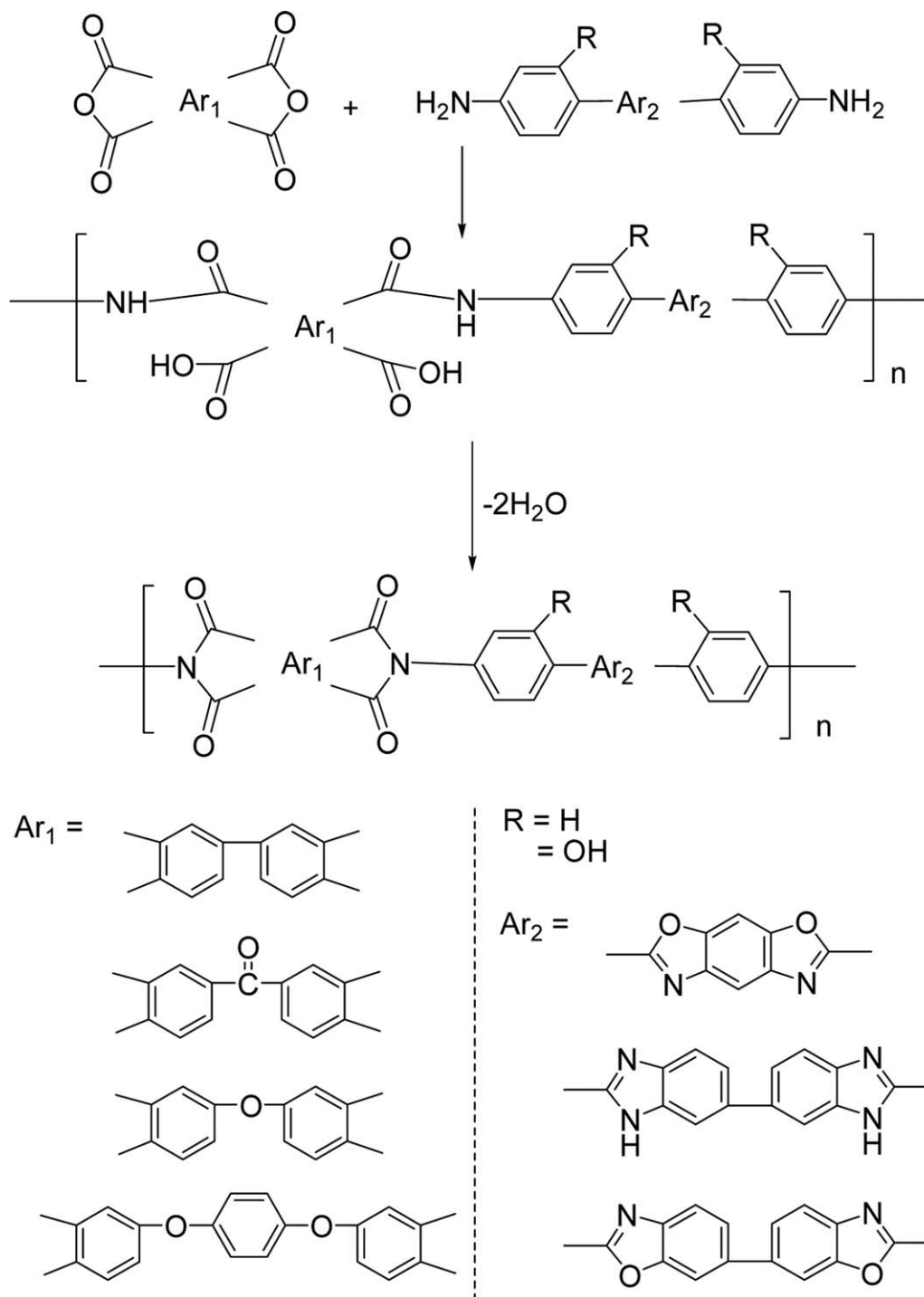
Five aromatic diamines containing benzimidazole, benzoxazole, and hydroxyl groups were synthesized according to a published method²⁸ by the reaction of 4-aminobenzoic acid or 4-aminosalicylic acid and monomer B in PPA with P_2O_5 , as shown in Scheme 1. PPA is widely used for catalyzing intramolecular cyclization reactions because of its high dehydration and low oxidizability. TOF-MS and ^1H and ^{13}C NMR spectroscopy were used to identify the structure of the target diamines. TOF-MS results showed the molecular weights of 342.1 (1-DA), 374.1 (1-OHDA), 418.1 (3-DA), 416.2 (2-DA), and 450.1 (3-OHDA), which were close to the theoretical values of the target products. The ^1H -NMR spectra are shown in Figure 1. The peaks at 11.07 (1-OHDA) and 11.13 ppm (3-OHDA) are assigned to the protons of hydroxyl groups. The peak at 12.46 ppm (2-DA) is assigned to the protons of the imidazole ring $-\text{NH}-$ group. The aromatic protons in the skeleton of 1-DA, 1-OHDA, 2-DA, 3-DA, and 3-OHDA molecules are located within the range of 6.69–8.05, 6.19–8.14, 6.66–7.87, 6.68–8.01, and 6.18–8.09 ppm, respectively, and the attribution of each proton is labeled in Figure 1. The protons of amino groups in the skeleton of 1-DA, 1-OHDA, 2-DA, 3-DA, and 3-OHDA molecules are located at 5.99, 6.09, 5.60, 5.99, and 6.11 ppm, respectively. ^{13}C NMR spectra exhibited 9

(1-DA), 11 (1-OHDA), 11 (3-DA), 7 (2-DA), and 13 (3-OHDA) peaks, all of which corresponding to the carbon atoms of the target product. The ^1H and ^{13}C NMR spectra indicate a consistent structure of the products with the target.

The polymerization of diamine and dianhydride involves the nucleophilic substitution reaction of amino group. The protons peak of amino group appear in low field in the ^1H -NMR spectra, the electron cloud density is lower, and the reactivity of diamine is also lower.²⁹ The results showed that the polymerization activities of diamines possibly decreased in the order of the diamines containing benzimidazole (2-DA) > the diamines containing benzoxazole (1-DA and 3-DA) > the diamines containing hydroxyl group and benzoxazole (1-OHDA and 3-OHDA).

Solution polymerization of diamines and various dianhydrides yielded viscous solution of PAAs. Thermal imidization

FIGURE 1 ^1H NMR spectra of diamines.



SCHEME 2 Synthesis of PIAs.

via a programmed heating procedure followed, as shown in Scheme 2. PAAs solution showed high inherent viscosities of 0.5 to 2.3 dL/g, as listed in Table 2. These samples produced flexible films, except 1-BPOHPI, by casting from the PAA solutions and thermal treatment. Considering that the diamine 1-OHDA possessed intramolecular H-bonding in comparison with 1-DA, and the molecule is fully rigid as shown Figure 4. Crystal precipitates appeared with the increase in polymeriza-

tion viscosity of 1-OHDA and BPDA. Consequently, the resulting film of 1-BPOHPI was brittle.

FT-IR Spectroscopic Studies

FT-IR spectroscopy is frequently used in the detection of H-bonding interactions, since IR is sensitive to the frequency shift of the proton donor and acceptor when H-bonding is formed.³⁰⁻³⁴ The strength of intermolecular interaction was

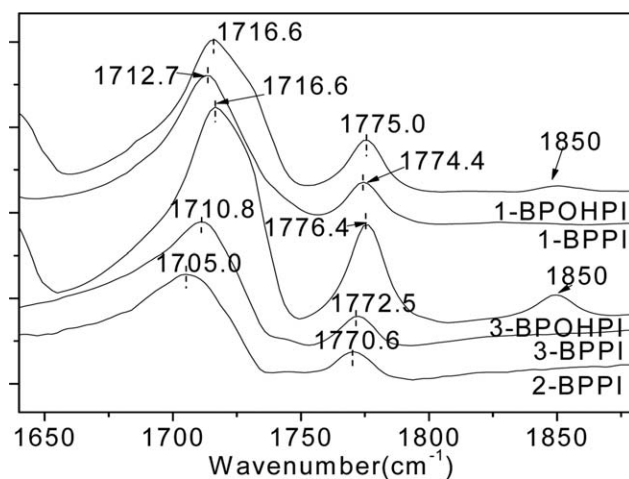


FIGURE 2 FT-IR spectra of the PIs.

investigated in terms of H-bonding by analyzing the frequency difference of C=O between difference diamines derived PIs. Figure 2 shows the FT-IR spectra of PIs prepared from BPDA. The peak positions of the symmetrical and asymmetrical C=O stretching vibration, which are characteristic of the imide ring, appeared in the vicinity of 1700 and 1770 cm^{-1} for all samples.

Given that the C=O group was expected to form H-bonding with —NH— and —OH groups due to the presence of the lone electron pair at the oxygen atom, the C=O band would be weaker than that whose electron was not transferred. Moreover, red shift would occur upon the formation of H-bonding. Compared with the C=O wave numbers of 1710.8 and 1772.5 cm^{-1} for 3-BPPI, the C=O wave numbers of 2-BPPI shifted to lower frequencies at 1705 and 1770 cm^{-1} , whereas the C=O wave numbers of 3-BPOHPI shifted to higher frequencies at 1716.6 and 1776.4 cm^{-1} , suggesting the H-bonding structural difference between 2-BPPI and 3-BPOHPI, as shown Figure 4. The imide C=O is a intermolecular H-bonding with the imidazole —NH— group for poly(benzimidazole imide) 2-BPPI, accordingly the C=O vibration occurred red shift than poly(benzoxazole imide) 3-BPPI.^{24,25} For the containing hydroxyl poly(benzoxazole imide) 3-BPOHPI, the hydroxyl group and oxazole nitrogen atom form intramolecular H-bonding to a large conjugated system, resulting in the enhanced inductive effect of imide ring nitrogen atom for the C=O group. Thus, the C=O vibration of 3-BPOHPI appeared in higher frequencies than those of 3-BPPI. The peak positions of the symmetrical and asymmetrical C=O stretching vibration appeared in the wave numbers of 1712.7 and 1774.4 cm^{-1} for 1-BPPI and 1716.6 and 1775.0 cm^{-1} for 1-BPOHPI, and the C=O stretching vibration of the hydroxyl-containing poly(benzoxazole imide) is also moved to a higher wave number. Meanwhile, we surmise that the small absorption at 1850 cm^{-1} for 3-BPOHPI and 1-BPOHPI caused by C=C-C=O groups formed by intramolecular H-bonding (Fig. 4) in the hydroxyl-containing poly(benzoxazole imide).³⁵

The FTIR spectra in the range of 1650–1750 cm^{-1} that belonged to Vas(C=O) of imide were carefully investigated to evaluate the evolution of H-bonding interactions. The curve-resolved FTIR spectra are displayed in Figure 3 for PIs, and four peaks are separately identified. Konicieczny and Wunder³⁶ reported that band IV (center: around 1690 cm^{-1}) is due to the asymmetric stretching of C=O. Bands III (center: 1703 cm^{-1}), band II (center: 1714 cm^{-1}), and band I (center: 1726 cm^{-1}) correspond to hydrogen-bonded C=O, van der Waals forces associated C=O, and “free” C=O stretching of the cyclic imides for poly(benzimidazole imide) (2-HPI), respectively.²⁵ Given the absence of H-bonding, band III is not present in poly(benzoxazole imide)s (1-HPI and 3-HPI). In the hydroxyl-containing poly(benzoxazole imide)s (1-HOHPI and 3-HOHPI), hydrogen-bonded C=O stretching band III also does not exist. For quantitative evaluation, the percentage of the C=O stretching bands was calculated and analyzed results are summarized in Table 1.^{37–39} The percentages of van der Waals forces associated C=O stretching band II were 51%, 61%, 52%, and 62% for 1-HPI, 1-HOHPI, 3-HPI, and 3-HOHPI, respectively. The values of hydroxyl-containing poly(benzoxazole imide)s (1-HOHPI and 3-HOHPI) were higher than those of poly(benzoxazole imide)s (1-HPI and 3-HPI). This result suggests that the hydroxyl-containing poly(benzoxazole imide)s have higher intermolecular force than their corresponding poly(benzoxazole imide)s.

Thermal Properties

The different intermolecular and intramolecular forces of PIs result in significant differences in their properties. The dynamic mechanical properties of PI films are investigated by DMA, and T_g was defined as the peak of $\tan \delta$ (Table 2). The PIs exhibited good thermal properties and all T_g except 3-HPI exceeded 300 °C because of the rigid rod structure of the nitrogen heterocyclic ring. The properties of PIs prepared from diamines (1-OHDA, 1-DA) and diamines (2-DA, 3-DA, and 3-OHDA) are comparable. The T_g values of the PIs are displayed in Figure 5. The T_g values of imidazole-containing diamine 2-DA derived PIs were the highest, reaching 421 °C for 2-BPPI, and this result can be regarded as the effect of strong intermolecular forces that the benzimidazole unit imparted.^{22,24} The T_g values of 3-OHDA derived PIs were higher than that of 3-DA derived PIs, and the T_g values of 1-OHDA derived PIs were higher than that of 1-DA derived PIs, which are due to the intermolecular and intramolecular H-bonding interaction of —OH groups. Another characteristic that was taken into account was the T_g difference (ΔT_g), which is listed in Table 3. The T_g differences, ΔT_{g1} , ΔT_{g2} , and ΔT_{g3} , between 1-OHDA and 1-DA, between 2-DA and 3-DA, and between 3-OHDA and 3-DA derived PIs ranged within 6–44 °C, 62–83 °C, and 22–39 °C, respectively, with the same dianhydride, and the ΔT_{g2} were highest. All characteristics showed that the PIs containing imidazole formed stronger intermolecular forces than the PIs containing hydroxyl and benzoxazole.

The thermal stability of PIs were analyzed using TGA, and the results are summarized in Table 2. All derived PIs exhibited good thermal stability. The 5% and 10% weight-loss

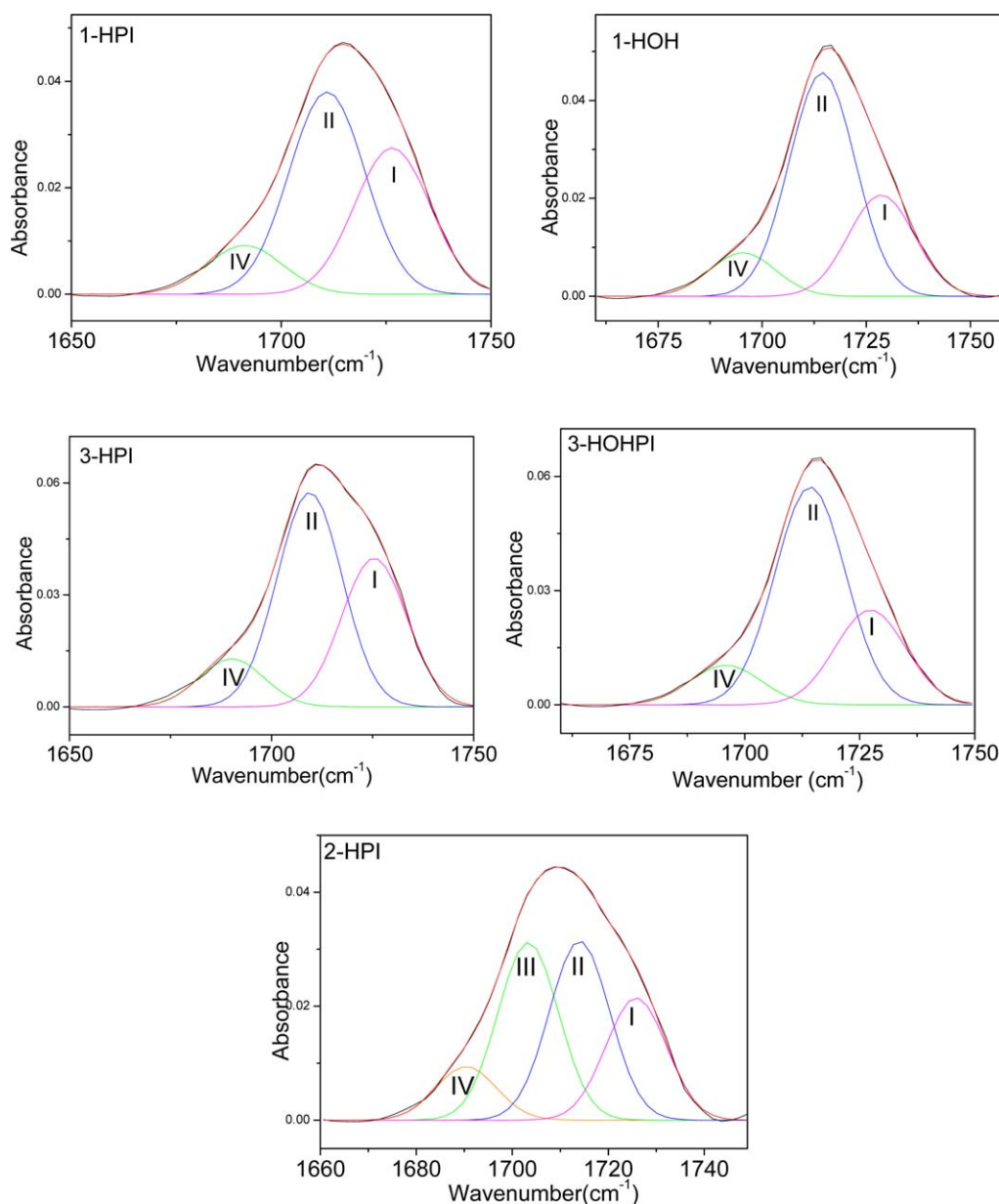


FIGURE 3 Curve-resolved FTIR spectra in the range of 1650–1750 cm^{-1} for Pls; Band I belongs to “free” C=O, Band II belongs to van der Waals forces associated C=O and Band III belongs to H-bonding associated C=O. [Color figure can be viewed in the online issue, which is available at wileyonlinelibrary.com.]

TABLE 1 Curve-Fitting Result of the FTIR Spectra in the Range of 1650–1750 cm^{-1} for Pls

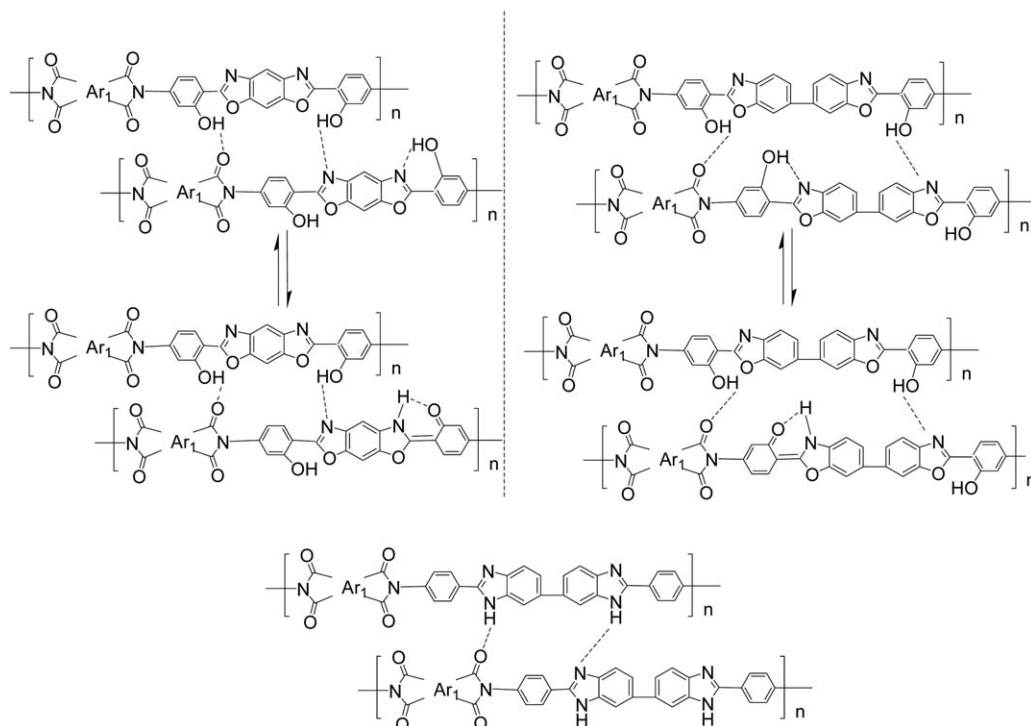
Pls	1-HPI		1-HOHPI		2-HPI		3-HPI		3-HOHPI	
	Freq (cm^{-1})	Area (%)								
Band I	1726	37	1729	27	1726	23	1725	36	1727	27
Band II	1711	51	1714	61	1714	34	1709	52	1714	62
Band III					1703	33				
Band IV	1691	12	1695	12	1690	10	1690	12	1696	11

TABLE 2 Inherent Viscosity (ζ_{inh}) and Properties of the PIs

PI	Diamines	Dianhydrides	η (dL/g)	T_g ($^{\circ}\text{C}$) ^a	T_{d5} ($^{\circ}\text{C}$) ^b	T_{d10} ($^{\circ}\text{C}$) ^c	Char Yield (%) ^d	CTE (ppm/ $^{\circ}\text{C}$)
1-BPPI	1-DA	BPDA	2.33	374	589	608	64	-6.4
1-BTPI	1-DA	BTDA	1.13	361	553	576	58	6.1
1-OPI	1-DA	ODPA	1.34	346	562	587	61	7.2
1-HPI	1-DA	HQDPA	1.70	302	555	572	57	10.2
1-BPOHPI	1-OHDA	BPDA	1.02	-	-	-	-	-
1-BTOHPI	1-OHDA	BTDA	0.77	367	533	561	59	4.0
1-OOHPI	1-OHDA	ODPA	0.89	358	553	574	59	3.3
1-HOHPI	1-OHDA	HQDPA	0.96	346	524	545	56	8.8
2-BPPI	2-DA	BPDA	1.03	421	485	574	71	-0.35
2-BTPI	2-DA	BTDA	0.81	397	512	557	72	10.1
2-OPI	2-DA	ODPA	0.80	387	521	571	70	9.0
2-HPI	2-DA	HQDPA	1.11	361	493	536	69	37.6
3-BPPI	3-DA	BPDA	2.26	338	579	599	67	4.9
3-BTPI	3-DA	BTDA	0.99	335	544	572	64	18.3
3-OPI	3-DA	ODPA	1.58	316	548	577	64	24.9
3-HPI	3-DA	HQDPA	1.30	296	535	557	62	42.3
3-BPOHPI	3-OHDA	BPDA	0.71 ^e	372	547	581	62	3.5
3-BTOHPI	3-OHDA	BTDA	0.55 ^e	357	538	569	64	17.0
3-OOHPI	3-OHDA	ODPA	0.61 ^e	355	521	558	60	23.2
3-HOHPI	3-OHDA	HQDPA	0.78 ^e	326	499	521	58	38.3

^a Peak temperature of $\tan \delta$ by DMA in nitrogen.^b Temperature at which a 5% weight loss was recorded by TGA.^c Temperature at which a 10% weight loss was recorded by TGA.^d Residual weight retention when heated to 800 $^{\circ}\text{C}$ in nitrogen.^e Inherent viscosities were measured in NMP.

- The 1-BPOHPI film is brittle.

**FIGURE 4** H-bonding in poly(benzimidazole imide) and poly(benzoxazole imide) (Refs. 24 and 34).

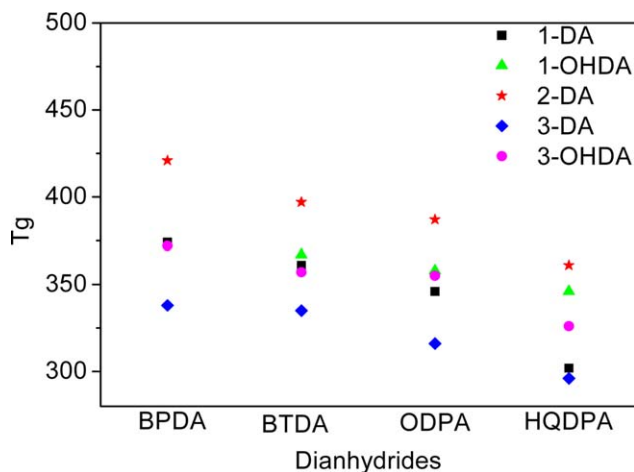


FIGURE 5 T_g values of PIs. [Color figure can be viewed in the online issue, which is available at wileyonlinelibrary.com.]

temperatures of the polymers were recorded as 485–589 °C and 521–608 °C, respectively. In addition, the Char yield of the PIs in nitrogen atmosphere at 800 °C were 56%–72%, as summarized in Figure 6. The Char yield of 2-DA prepared PIs were the highest within 69%–72%, the finding are due to the following: (1) the strong H-bonding of the imidazole group, which functions as physical crosslinking and increases the contact between molecular chains, and (2) the higher proportion of nitrogen in the molecule. The Char yield of hydroxyl-containing poly(benzoxazole imide)s were slightly lower than their corresponding poly(benzoxazole imide)s because of the hydroxyl degradation. In general, the different thermal stabilities of the polymers were related to their compositions and structures, the existence of highly rigid benzoxazole and benzimidazole leads to the increase in the thermal stability of PIs.

Dimensional Stability

The rigidity of the PI backbone would be considerably enhanced after the employment of benzoxazole and benzimidazole, as can be seen from the outstanding thermal resistance. Dimensional stability was expected to be improved. The thermal expansion coefficient (CTE) values were directly measured by the TMA instrument, and CTE values are shown in Figure 7. The PIs prepared from diamines 1-DA and 1-OHDA presented low CTE values of below 10 ppm/°C because of the fully rigid diamines containing

TABLE 3 ΔT_g of Polyimides

	ΔT_{g1}	ΔT_{g2}	ΔT_{g3}
BPDA	–	83	34
BTDA	6	62	22
ODPA	12	71	39
HQDDPA	44	65	30

T_g difference (ΔT_{g1} , ΔT_{g2} , and ΔT_{g3}) between 1-OHDA and 1-DA, between 2-DA and 3-DA and between 3-OHDA and 3-DA derived PIs with the same dianhydride.

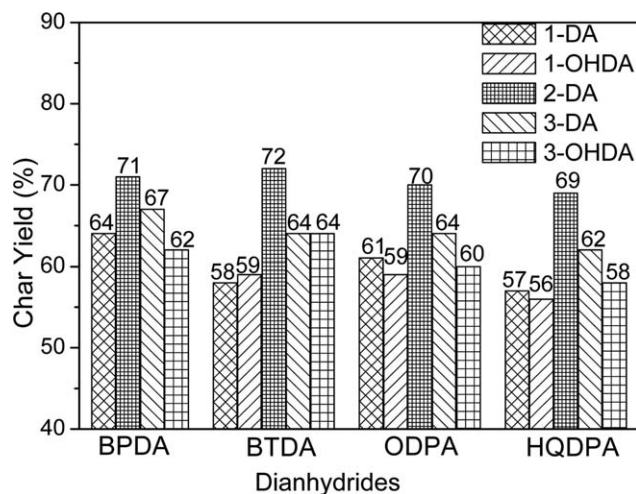


FIGURE 6 Char yield of PIs.

the benzobisoxazole unit. Given enhanced molecular chain rigidity and intermolecular force because of the intra-/intermolecular H-bonding of hydroxyl groups as shown Figure 4, the movement and rotation of molecular chains are limited, leading to the lower CTE value of 1-OHDA prepared PIs than that of 1-DA prepared PIs.

In comparing PIs prepared from 2-DA, 3-DA, and 3-OHDA, we can see that the CTE values of 3-OHDA derived hydroxyl-containing poly (benzoxazole imide)s were lower than 3-DA derived poly(benzoxazole imide)s. However, the CTE values of 2-DA derived poly(benzimidazole imide)s were the lowest. The strong H-bonding of imidazole was speculated to perform a physical crosslinking function, and the intermolecular H-bonding interaction of imidazole was stronger than the hydroxyl group. Among all PIs, low CTE is observed due to their rigid rod-like characteristics imparted by benzoxazole and benzimidazole.

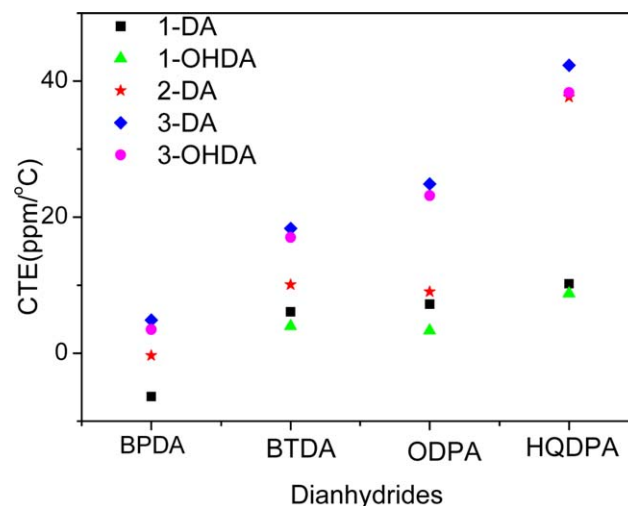


FIGURE 7 CTE of PIs. [Color figure can be viewed in the online issue, which is available at wileyonlinelibrary.com.]

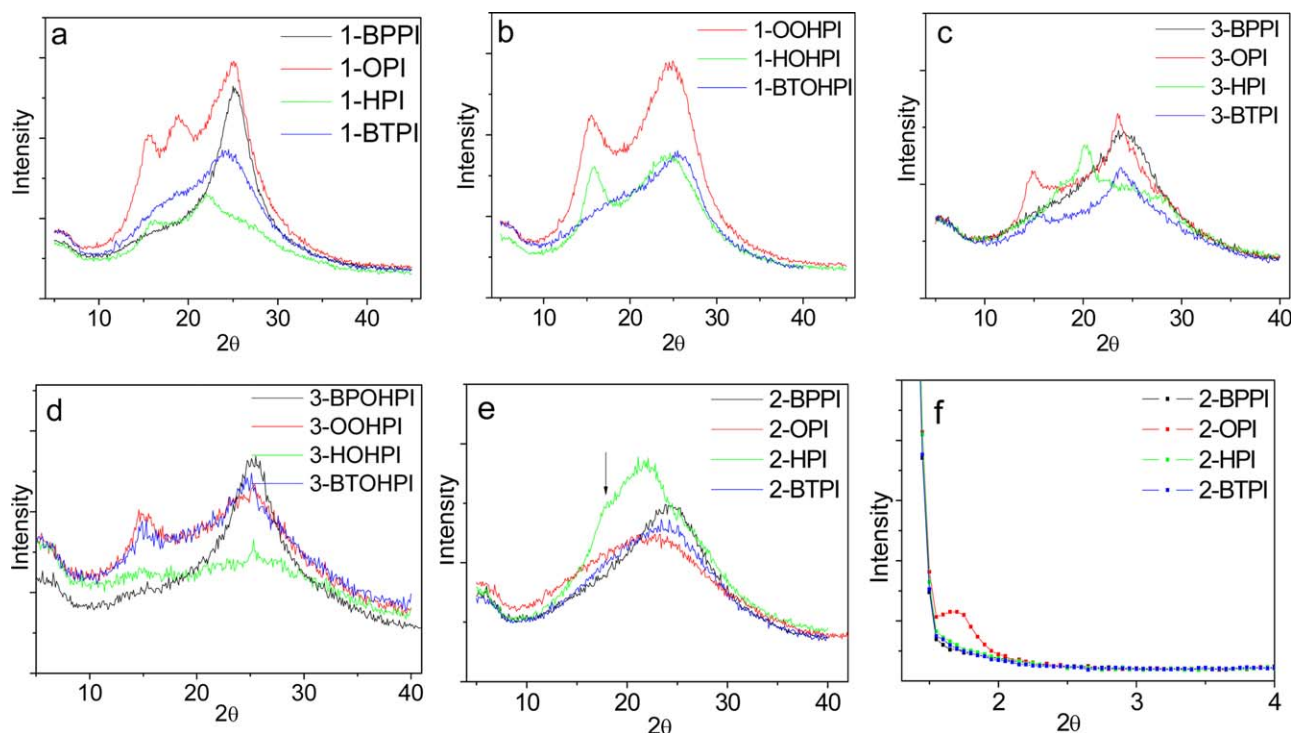


FIGURE 8 XRD patterns of PIs. [Color figure can be viewed in the online issue, which is available at wileyonlinelibrary.com.]

Aggregation State

The morphological structures of PI films were examined by XRD, as shown in Figure 8. The XRD curves show ordered structures around $2\theta = 15^\circ$ ($d = 5.9 \text{ \AA}$), 18° ($d = 4.9 \text{ \AA}$), and 25° ($d = 3.6 \text{ \AA}$) for 1-DA [Fig. 8(a)], 1-OHDA [Fig. 8(b)], 3-DA [Fig. 8(c)], and 3-OHDA [Fig. 8(d)] derived poly(benzoxazole imide)s, which indicate crystalline morphology. The crystalline structure should be related to rigidity and planar structure of benzoxazole, which enables the effective packing of molecular chains, particularly for 1-DA and 1-OHDA containing benzobisoxazole units.

The 2-DA derived poly(benzimidazole imide) films were essentially amorphous, as can be deduced from the broad patterns in the diagrams of Figure 8(e). However, signs of crystallization were observed, as demonstrated by the presence of discrete diffraction peaks in the diagrams of Figure 8(e) (2-HPI) and Figure 8(f) (2-OPI). In addition, diffraction peaks (2θ) were located at 18° and 1.67° for 2-HPI and 2-OPI, respectively, and d spacing could be calculated as 4.9 \AA for 2-HPI and 52 \AA for 2-OPI. Considering that the d spacing obtained from XRD reflections corresponds to interchain Packing,^{40–42} the result indicated that the long period, the average distance between the ordered regions, was shorter for 2-HPI because of its greater flexibility than 2-OPI.

The morphological structures of poly(benzimidazole imide) films were further measured using the SAXS measurements as presented in Figure 9. A peak at around $q = 0.34 \text{ nm}^{-1}$, which corresponded to a periodic distance of 18.5 nm , was observed for 2-HPI films. In 2-BPPI, 2-BTPI, and 2-OPI films,

the scattering peaks appeared at around $q = 1.2 \text{ nm}^{-1}$. The calculated d spacing was 52 \AA , which corresponded to the long period of the 2-OPI film detected by the XRD test. These results indicate that the periodical lamellar structure formed in poly(benzimidazole imide) films.

For poly(benzoxazole imide)s and hydroxyl-containing poly(-benzoxazole imide)s, given the rigid rod-like structure of benzoxazole and relatively weak intermolecular H-bonding

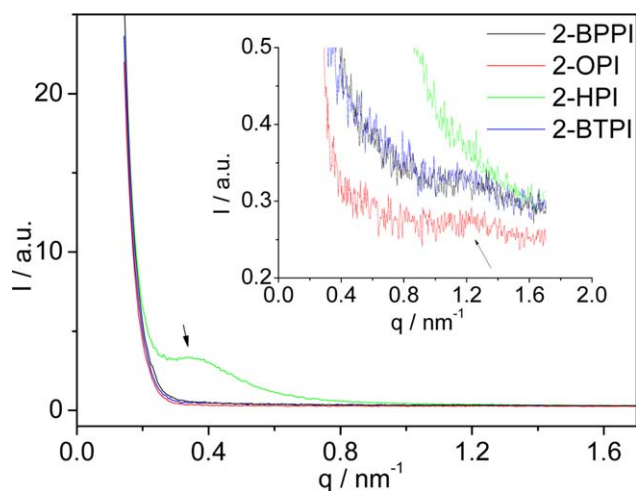


FIGURE 9 SAXS patterns of poly(benzimidazole imide) films. [Color figure can be viewed in the online issue, which is available at wileyonlinelibrary.com.]

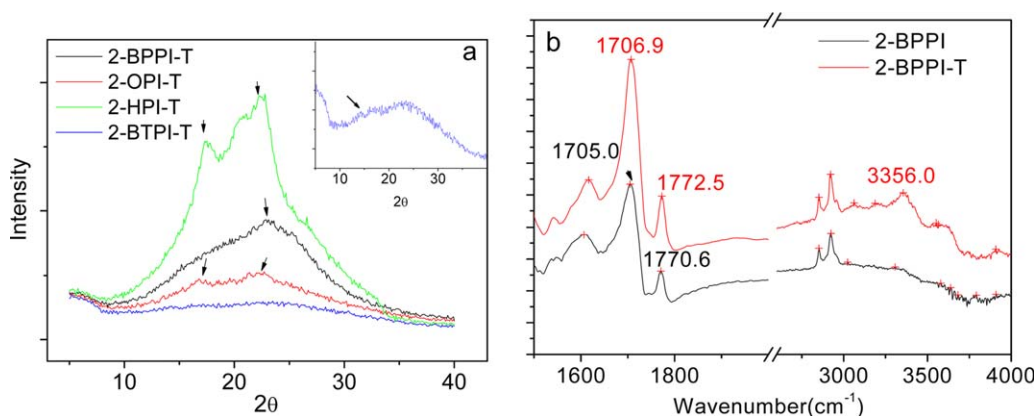


FIGURE 10 XRD patterns (a) and FTIR spectra (b) of the poly(benzimidazole imide) films after heat treatment at 400 °C/2 h. [Color figure can be viewed in the online issue, which is available at wileyonlinelibrary.com.]

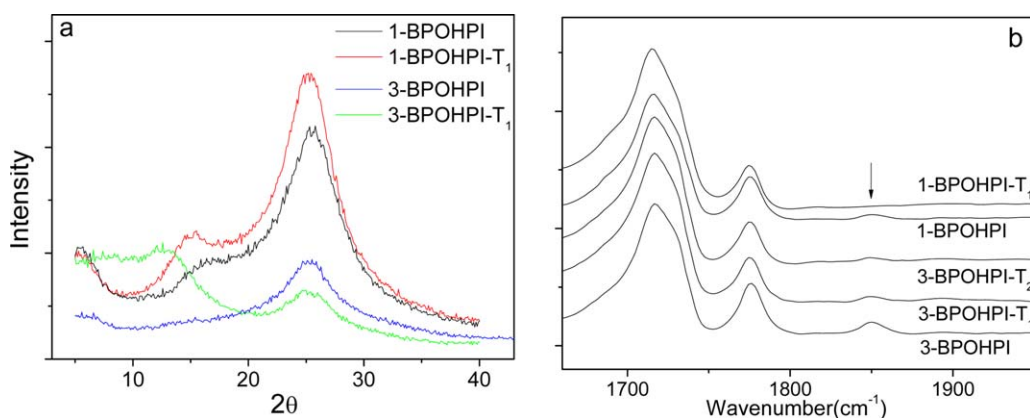


FIGURE 11 XRD patterns (a) and FTIR spectra (b) of hydroxyl-containing poly(benzoxazole imide) films after heat treatment at T_1 (400 °C/4 h) and T_2 (400 °C/8 h). [Color figure can be viewed in the online issue, which is available at wileyonlinelibrary.com.]

interactions, the molecular chain can move, rearrange, and consequently form stable crystalline structures below 350 °C (imidization temperature). For poly(benzimidazole imide)s, the motion and rotation of molecular chain are difficult because of strong intermolecular forces of the imidazole group, so the formation of a crystalline structure is impeded, the periodical ordered structure and weak crystallization appeared below 350 °C (imidization temperature).

Effects of Heat Treatment

The morphological structures of PI films are known to be strongly influenced by annealing temperatures.⁴³ Poly (benzimidazole imide) films were denoted as 2-BPPI-T, 2-BTPI-T, 2-OPI-T, and 2-HPI-T after heat treatment at 400 °C for 2 h. According to the XRD patterns in Figure 10(a), signs of crystallization were observed around $2\theta = 17^\circ$ ($d = 5.2$ Å) and $2\theta = 23^\circ$ ($d = 3.9$ Å), and crystallinity increased than before heat treatment. According to the FTIR spectra in Figure 10(b), the carbonyl stretching vibration (1770.6 and 1705 cm^{-1}) of 2-BPPI was increased to (1772.5 and 1706.9 cm^{-1}) of 2-BPPI-T, respectively. The vibration peak at 3356 cm^{-1} was enhanced, it is attributed to the characteristic peak of imidazole —NH— . These results manifest that the part of H-bonding between the imidazole and carbonyl was

overcome at higher temperature (400 °C). Moreover, intermolecular forces were weakened and the motion of molecule chain becomes free. Then the macromolecular packing becomes more orderly and the crystalline structure appears.

1-BPOHPI and 3-BPOHPI films were denoted as 1-BPOHPI-T and 3-BPOHPI-T, after heat treatment at 400 °C. The crystallinity increased than before heat treatment, as seen in the XRD patterns in Figure 11(a). The IR spectra [Fig. 11(b)] shows that the vibration peaks at 1850 cm^{-1} were weakened or disappeared after heat treatment at 400 °C, indicating the destruction of intramolecular H-bonding.

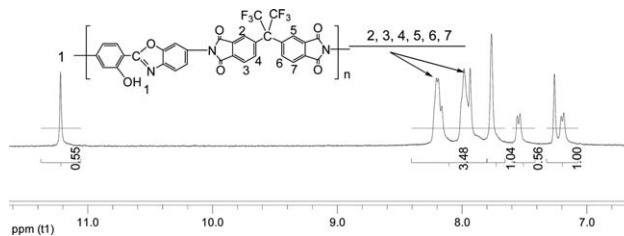


FIGURE 12 ^1H NMR spectrum of soluble FOHPI after heat treatment at 350 °C/6 h.

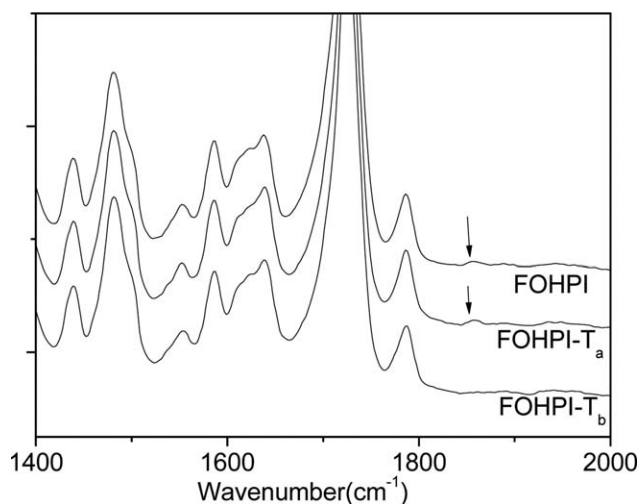


FIGURE 13 FTIR spectra of soluble FOHPI film after heat treatment at T_a (350 °C/6 h) and T_b (400 °C/4 h).

To further investigate the effects of heat treatment on hydroxyl-containing poly(benzoxazole imide), the soluble hydroxyl-containing poly(benzoxazole imide) FOHPI (For complete experimental details of the FOHPI refer to the Supporting Information) shown in Figure 12 was prepared. The IR spectra as seen Figure 13 display that the vibration peak of intramolecular H-bonding at 1857 cm^{-1} did not change after heat treatment at 350 °C for 6 h. The PI was soluble in the solvent DMSO, but extremely few gels were produced after heat treatment at 350 °C for 6 h. In the $^1\text{H-NMR}$ spectrum shown in Figure 12, the peak at 11.23 ppm was assigned to the protons of hydroxyl groups. The proportion for each integral area of peaks was 0.55:3.48:1.04:0.56:1.00, which was in good accordance with the theoretical values of 1:7:2:1:2, these phenomena showed that the hydroxyl group and the chain structure of FOHPI did not change after heat treatment at 350 °C. The vibration peak at 1857 cm^{-1} disappeared with the change of the heat treatment to 400 °C, indicating that intramolecular hydrogen bonds were destroyed, whereas FOHPI became insoluble in the solvent DMSO. Thus, we speculate that hydroxyl-containing poly(benzoxazole imide)s were formed in the crosslinking structures after heat treatment at 400 °C because of the hydroxyl degradation.⁴⁴

CONCLUSIONS

PIs containing benzimidazole, benzoxazole, and hydroxy groups were prepared, and the influence of H-bonding on the properties of PIs was investigated. The results are summarized as follows. (1) PIs containing nitrogen heterocycles present high thermal properties; for example, the T_g of 2-BPPI containing benzimidazole reached 421 °C. (2) By comparing the properties of PIs, we found that hydroxyl-containing poly(benzoxazole imide)s present higher T_g values and dimensional stabilities than their corresponding poly(benzoxazole imide)s. (3) These corresponding poly(benzimidazole imide)s exhibited the best performances, such as the highest T_g , the highest char yield and the highest dimen-

sional stabilities. These results showed that the H-bonding effect of benzimidazole is stronger than that of hydroxyl groups. (4) Poly(benzoxazole imide)s show crystalline structure, whereas poly(benzimidazole imide)s show amorphous state or weak ordered structure, after imidization at 350 °C. Intermolecular H-bonding interactions were overcome for poly(benzimidazole imide)s after heat treatment at 400 °C, the molecular chains were rearranged and the crystalline structures were formed. (5) Hydroxyl-containing poly(benzoxazole imide)s were formed in crosslinking structures after heat treatment at 400 °C. The results of this study contribute in designing a material with specific properties according to the structure–property relationship.

ACKNOWLEDGMENTS

The financial support from the National Nature Science Foundation of China (21104085) and the National High Technology Research and Development Program of China (863 Program no. 2012AA03A211) and Supported by Major State Basic Research Development Program (973 Program no. 2014CB643603) is gratefully acknowledged.

REFERENCES AND NOTES

- 1 C. E. Sroog, *Prog. Polym. Sci.* **1991**, *16*, 561–694.
- 2 D. Wilson, H. D. Stenzenberger, P. M. Hergenrother, *Polyimides*; Chapman & Hall: New York, **1990**.
- 3 M. K. Ghosh, K. L. Mittal, *Polyimides: Fundamentals and Applications*; Marcel Dekker: New York, **1996**.
- 4 M. Hasegawa, K. Horie, *Prog. Polym. Sci.* **2001**, *26*, 259–335.
- 5 A. Xia, H. Guo, X. Qiu, M. Ding, L. Gao. *J. Appl. Polym. Sci.* **2006**, *102*, 1844–1851.
- 6 C. Arnold, *J. Polym. Sci. Macromol. Rev.* **1979**, *14*, 265–378.
- 7 J. F. Wolfe, F. E. Arnold, *Macromolecules* **1981**, *14*, 909–915.
- 8 D. N. Khanna. U.S. Patent 5,071,948, **1991**.
- 9 W. J. Harris, W. F. Hwang. U.S. Patent 5,985,969, **1999**.
- 10 G. S. Liou, *J. Polym. Sci., Part A: Polym. Chem.* **1999**, *37*, 4151–4158.
- 11 Y. Sakaguchi, Y. Kato, *J. Polym. Sci., Part A: Polym. Chem.* **1993**, *31*, 1029–1033.
- 12 M. Bruma, F. Mercer, B. Schulz, R. Dietel, W. Neumann, *Polym. Adv. Technol.* **1994**, *5*, 535–540.
- 13 R. A. Sunder, L. J. Mathias, *J. Polym. Sci., Part A: Polym. Chem.* **1994**, *32*, 2825–2839.
- 14 J. L. Hedrick, T. P. Russell, J. W. Labadie, J. G. Hilborn, T. D. Palmer, *Polymer* **1990**, *31*, 2384–2392.
- 15 S. Hsu, H. T. Chen, S. J. Tsai. *J. Polym. Sci., Part A: Polym. Chem.* **2004**, *42*, 5990–5998.
- 16 E. Hamciuc, M. Bruma, F. W. Mercer, C. I. Simionescu, *Angew. Makromol. Chem.* **1993**, *210*, 143–150.
- 17 M. Berrada, Z. Anbaoui, N. Lajrhed, M. Berrada, N. Knouzi, *Chem. Mater.* **1997**, *9*, 1989–1993.
- 18 I. S. Chung, C. E. Park, M. Ree, S. Y. Kim, *Chem. Mater.* **2001**, *13*, 2801–2806.
- 19 M. Berrada, F. Carriere, Y. Abboud, A. Abourriche, A. Benamara, N. Lajrhed, M. Kabbaj, M. Berrada, *J. Mater. Chem.* **2002**, *12*, 3551–3559.

- 20** J. Liu, Q. Zhang, Q. Xia, J. Dong, Q. Xu, *Polym. Degrad. Stab.* **2012**, *97*, 987–994.
- 21** G. Song, S. Wang, D. Wang, H. Zhou, C. Chen, X. Zhao, G. Dang, *J. Appl. Polym. Sci.* **2013**, *130*, 1653–1658.
- 22** S. Wang, H. Zhou, G. Dang, C. Chen, *J. Polym. Sci., Part A: Polym. Chem.* **2009**, *47*, 2024–2031.
- 23** Y. Zhuang, X. Liu, Y. Gu, *Polym. Chem.* **2012**, *3*, 1517–1525.
- 24** G. Song, Y. Zhang, D. Wang, C. Chen, H. Zhou, X. Zhao, G. Dang, *Polymer* **2013**, *54*, 2335–2340.
- 25** L. Luo, J. Yao, X. Wang, K. Li, J. Huang, B. Li, H. Wang, Y. feng, X. Liu, *Polymer* **2014**, *55*, 4258–4269.
- 26** S. Jenkins, K. I. Jacob, S. Kumar, *J. Polym. Sci., Part B: Polym. Phys.* **2000**, *38*, 3053–3061.
- 27** D. J. Sikkema, In High-performance fibres; J. W. S. Hearle, Ed.; Woodhead Publishing Ltd and CRC Press LLC : Boca Raton, **2001**; Chapter 4, pp 108–115.
- 28** J. Preston, W. Dewinter, W. L. Hofferbert, *J. Heterocyclic Chem.* **1968**, *5*, 269–273.
- 29** M. X. Ding, Polyimide: Chemistry, Relationship Between Structure, and Properties and Materials; Science Press: Beijing, **2006**; Chapter 2, pp 11–16.
- 30** C. Zhang, J. Hu, D. Chen, Y. Zhu, Y. Fan, Y. Liu, *Polymer* **2012**, *53*, 4718–4726.
- 31** C. Lin, J. Kuo, C. Chen, J. Fang, *Polymer* **2012**, *53*, 254–258.
- 32** C. Lin, J. Kuo, C. Chen, *Eur. Polym. J.* **2000**, *36*, 1183–1193.
- 33** H. Dong, Z. Xin, X. Lu, Y. Lv, *Polymer* **2011**, *52*, 1092–1101.
- 34** A. Martinez-Felipe, Z. Lu, P. A. Henderson, S. J. Picken, B. Norder, C. T. Imrie, A. Ribes-Greus, *Polymer* **2012**, *53*, 2604–2612.
- 35** Q. Chu, D. A. Medvetz, Y. Pang, *Chem. Mater.* **2007**, *19*, 6421–6429.
- 36** J. M. Konieczny, S. L. Wunder, *Macromolecules* **1996**, *29*, 7613–7615.
- 37** P. Musto, F. E. Karasz, W. J. Macknight, *Macromolecules* **1991**, *24*, 4762–4769.
- 38** J. Dong, C. Yin, Z. Zhang, X. Wang, H. Li, Q. Zhang, *Macromol. Mater. Eng.* **2014**, *299*, 1170–1179.
- 39** H. Niu, M. Huang, S. Qi, E. Han, G. Tian, X. Wang, D. Wu, *Polymer* **2013**, *54*, 1700–1708.
- 40** M. Kotera, B. Samyul, K. Araie, Y. Sugioka, T. Nishino, S. Maji, M. Noda, K. Senoo, T. Koganezawa, I. Hirozawa, *Polymer* **2013**, *54*, 2435–2439.
- 41** M. Ree, K. Kim, S. H. Woo, H. Chang, *J. Appl. Phys.* **1997**, *81*, 698–708.
- 42** L. Shao, T. S. Chung, G. Wensley, S. H. Goh, K. P. Pramoda, *J. Membr. Sci.* **2004**, *244*, 77–87.
- 43** M. Hasegawa, N. Sensui, Y. Shindo, R. Yokota, *Macromolecules* **1999**, *32*, 387–396.
- 44** J. H. Hodgkin, M. S. Liu, B. N. Dao, J. Mardel, A. J. Hill, *Eur. Polym. J.* **2011**, *47*, 394–400.